Effect of Protonation and Deprotonation on the Gas-Phase Reactivity of Fluorinated 1,2,4-Triazines

Gianluca Giorgi,[a] Antonio Palumbo Piccionello,[b] Andrea Pace,[b] and Silvestre Buscemi[b]

[a] Dipartimento di Chimica, Università degli Studi di Siena, Siena, Italy
[b] Dipartimento di Chimica Organica "E. Paternò", Università degli Studi di Palermo, Palermo, Italy

Positive and negative electrospray mass spectrometry (MS), in-time and in-space MS^n experiments, high-resolution and accurate mass measurements obtained with an Orbitrap, together with density functional theory calculations have been used to study the gas-phase ion chemistry of a series of fluorinated 1,2,4-triazines. As a result of low-energy collision-induced dissociations, occurring in an ion trap and in a triple quadrupole, their protonated and deprotonated molecules show interesting features depending on the nature and structure of the precursor ions. The occurrence of elimination/hydration reactions produced by positive ions in the ion trap is noteworthy. Decompositions of deprotonated molecules, initiated by elimination of a hydroxyl radical from $[M-H]^-$, are dominated by radical anions. Theoretical calculations have allowed us to obtain information on atom sites involved in the protonation and deprotonation reactions. (J Am Soc Mass Spectrom 2008, 19, 686–694) © 2008 American Society for Mass Spectrometry

Triazines constitute a class of interesting compounds that find their applications in several fields, such as pharmaceutical chemistry [1], phytochemistry [2], biology [3, 4], catalysis [5], and supramolecular chemistry [6].

In the last decades different synthetic approaches have been set up for obtaining new fluorinated heterocyclic compounds [7]. Recently, we developed a new synthetic procedure for preparing series of fluorinated 1,2,4-triazines through ANRORC (addition of nucleophile, ring-opening, and ring-closure) rearrangements of 5-perfluoroalkyl-1,2,4-oxadiazoles [8].

In the framework of research aimed at studying the gas-phase ion chemistry of heterocyclic molecules [9], we seek to present here a mass spectrometry (MS) and a theoretical study of compounds **1–4** (Scheme **1**).

These compounds are particularly suitable and interesting for their gas-phase ion chemistry because they can be protonated or deprotonated by using electrospray ionization (ESI). It follows that it is possible to evaluate the effects of protonation and deprotonation on their gas-phase decompositions. Multiple MS separation stages arising from low-energy collision-induced dissociations (CIDs) occurring both in an ion trap (IT) and in a triple quadrupole (QqQ) mass spectrometer have been carried out and compared. High-resolution and accurate mass measurements, obtained by using an Orbitrap analyzer, have allowed us to determine the elemental composition for each ionic species detected in MS and MS^n spectra as a result of electrospray ionization. Because in each molecule different atoms might be involved in proton addition or abstraction, density functional theory (DFT) calculations have been carried out on different structures of protonated and deprotonated molecules of compound **1**.

Experimental

Synthesis of the Compounds and Mass Spectrometry

Compounds **1–4** were prepared according to the procedure described in Buscemi et al. [8, 10].

Electrospray measurements were carried out on an LCQ-DECA ion trap and on an LTQ-XP-Orbitrap instrument (Thermo Fisher Scientific, Bremen, Germany). Operating conditions of the ESI source were as follows: spray voltage, 4.5 kV; capillary temperature, 200 °C; sheath gas (nitrogen) flow rate, approximately 0.75 L min^{-1}. Ultrapure helium was the collision gas; CID collision energy: 0.5–1.0 eV (laboratory frame). The Orbitrap analyzer was operating in the resolution range 30,000–100,000 and calibrated using the manufacturer's calibration mixture. Mass accuracies <2 ppm were determined before and after each session of experiments. In all, 30–50 scans were recorded and averaged for accurate mass measurements.

Address reprint requests to Dr. Gianluca Giorgi, Università di Siena, Dipartimento di Chimica, via Aldo Moro, 53100 Siena, Italy. E-mail: gianluca.giorgi@unisi.it

1044-0305/08/$32.00
doi:10.1016/j.jasms.2008.01.014

Published online February 7, 2008
Received November 19, 2007
Revised January 28, 2008
Accepted January 28, 2008

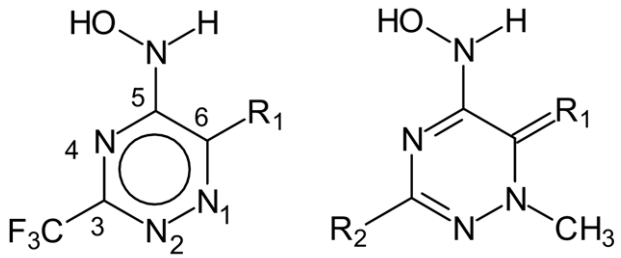

1. R_1=OH **3.** R_2=CF_3

2. R_1=Ph **4.** R_2=C_3F_7

Scheme 1.

Electrospray triple quadrupole measurements were carried out on a VG-Quattro LC (Waters, Manchester, UK) mass spectrometer. Spray voltage was 3.5 kV; the sampling cone was set at 5 V; and the counter-electrode potential was 500 V. The source temperature was 80 °C. Nitrogen was used as nebulizer and drying gas at flow rates of 60 and 400 L h^{-1}, respectively. CID experiments were carried out using argon as target gas at a pressure of about 1.4×10^{-3} bar. The laboratory energy was in the 20- to 25-eV range.

Working solutions were introduced into each mass spectrometer using a syringe pump at a flow rate of 5 μL min^{-1}.

The reported values of relative intensities in MS/MS spectra are the mean of 20–50 scans.

Theoretical Calculations

Density functional theory calculations were performed on different structures proposed for protonated and deprotonated molecules by using Gaussian 03 [11], implemented on an IBM SP RS/6000 Power 5 supercomputer at Cineca in Bologna, Italy. All geometries were fully optimized without any constraints at the Becke 3LYP (B3LYP) [12] method with the 6-31G(d,p) level of theory. The final lowest energy geometries were confirmed as a minimum on the potential energy surface by normal-mode vibrational frequency calculations that produced all real frequencies. Zero-point energies and statistical thermodynamic properties at 298.15 K and 1 atm were calculated at the B3LYP-6-31G(d,p) level of theory. A scaling factor of 0.9613 was used for zero-point energies [13].

Results and Discussion

*Gas-Phase Behavior of Protonated Molecules of Compounds **1–4***

The ESI (+) mass spectra of compounds **1–4** are characterized by protonated molecules and sodium adducts, whereas no other fragment ion is detected.

DFT calculations carried out on $[\mathbf{1}+H]^+$ cations, protonated at different sites, suggest that protonation on nitrogen atoms is highly favored, with N(2) being the preferred site, followed by N(4) and N(1) (Figure 1, Table 1).

Product ion CID spectra obtained in the ion trap by selecting the species $[M+H]^+$ of compounds **1–4** show common interesting features (Figure 2). The presence of puzzling ions that differ 2, 22, and 24 u from their precursors and that of clusters of ions that differ 2 u from each other [14] is noteworthy. As an example, the product ion MS/MS spectrum of $[\mathbf{1}+H]^+$ (*m/z* 197, Figure 2, top) shows the presence of ions at *m/z* 195, differing 2 u from the precursor ion. Other groups of ions differing 2 u from each other are also present at *m/z* 173, 175, 177, and at *m/z* 155, 157. Among them, ionic species at *m/z* 173, which differ 24 u from $[\mathbf{1}+H]^+$, are the most intense (Figure 2, top). This behavior can be explained by the occurrence of hydration/elimination reactions of trapped protonated molecules, mainly consisting of successive eliminations of HF followed by nucleophilic addition of water present in the ion trap [14].

This behavior resembles that recently observed for protonated bisubstituted isoquinolines that, when submitted to MS^3 and MS^4 experiments in an ion trap, show nominal elimination of 11 u, due to the loss of HCN and concomitant addition of oxygen [15].

For compounds **1–3**, the reaction pathways occurring as a result of CID are initiated by loss of HF from the protonated molecule, thus forming a carbocation $[(M+H)-20]^+$. The loss of HF is promoted by the protonation at N(2) that theoretical calculations suggest as the most favorable protonation site. A successive loss of HF produces the ions $[(M+H)-40]^+$. Alternatively, the species $[(M+H)-20]^+$ can add, through a 1,3-nucleophilic addition, a water molecule yielding the cation $[(M+H)-2]^+$. A further elimination of one or two molecules of HF yields ions formally due to $[(M+H)-22]^+$ and $[(M+H)-42]^+$, respectively. This latter can add another molecule of water, thus producing the species $[(M+H)-24]^+$.

Protonated molecules can also decompose by elimination of a water molecule followed by HF, thus producing ions $[(M+H)-18]^+$ and $[(M+H)-38]^+$, respectively. These latter can undergo a hydration reaction yielding the species $[(M+H)-20]^+$, whose reactivity was reported earlier. Elemental compositions of all these ionic species have been confirmed by accurate mass measurements carried out under high-resolution conditions.

Gas-phase decompositions strictly dependent on the chemical structure of the ions are also observed. One example is the fragmentation pathway that yields ions at *m/z* 151 in the IT-MS^2 spectrum of $[\mathbf{1}+H]^+$ (Figure 2, top). Accurate mass measurements have allowed us to determine that their elemental composition is $C_3H_2N_4F_3$ (calcd 151.0226, measured 151.0224), indicating a nom-

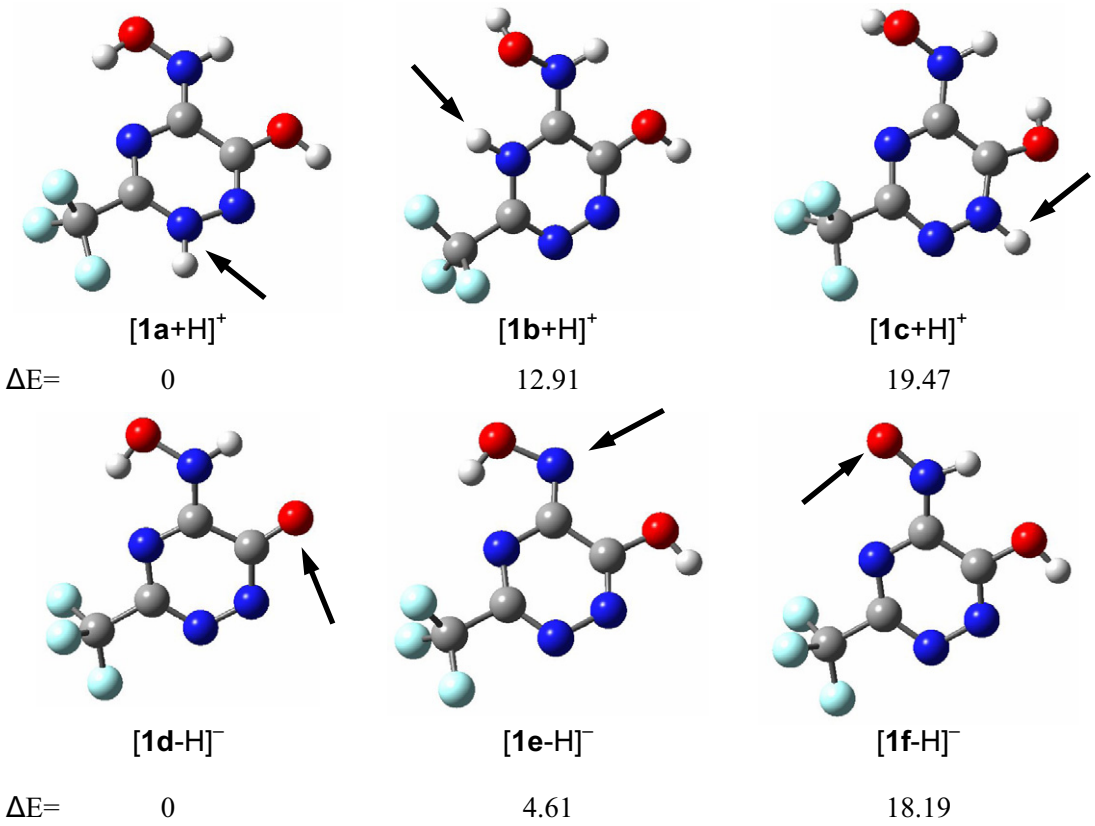

Figure 1. Energy-minimized structures for protonated (top row) and deprotonated (bottom row) molecules of compound **1**. Arrows indicate the protonation/deprotonation site. ΔE values are in kcal mol^{-1}.

inal loss of CH_2O_2 from the protonated molecule. This loss might be ascribed to the elimination of formic acid, but it seems unlikely because it should require deep rearrangements. Thus we propose that ions at *m/z* 151 are produced by consecutive losses of water and CO from $[\mathbf{1}+H]^+$.

As a result of low-energy collision-induced dissociations occurring in the ion trap, the protonated species $[\mathbf{2}+H]^+$ (*m/z* 257) shows an abundant elimination of a water molecule. Distinctive fragmentation pathways, observed in MS^3 experiments by selecting the cation $[(\mathbf{2}+H)-H_2O]^+$ as precursor ion, yield the species

Table 1. Energy values of minimized species produced by **1**

Species	B3LYP 6-31G(d,p)[a]	ZPVE[b]	SCF + ZPVE[a]	ΔE (SCF + ZPVE)[c]
$[\mathbf{1a}+H]^+$	−823.489023	0.104296	−823.384727	0
$[\mathbf{1b}+H]^+$	−823.467561	0.103416	−823.364145	12.91
$[\mathbf{1c}+H]^+$	−823.456856	0.103158	−823.353698	19.47
$[\mathbf{1d}-H]^-$	−822.587675	0.078325	−822.509350	0
$[\mathbf{1e}-H]^-$	−822.580493	0.078488	−822.502005	4.61
$[\mathbf{1f}-H]^-$	−822.558682	0.078321	−822.480361	18.19

[a]Units of Hartree.
[b]Zero-point vibrational energies corrected by 0.9613 [13]; units of Hartree/particle.
[c]kcal mol^{-1}.

$[(\mathbf{2}+H-H_2O)-HF-N_2]^+$ and $[(\mathbf{2}+H-H_2O)-CF_3CN]^+$ at *m/z* 191 and 144, respectively, whose elemental compositions have been confirmed by accurate mass measurements.

Compound **4**, bearing a —C_3F_7 moiety at position 3 of the triazine ring, has a different behavior. In fact the IT-MS^2 spectrum obtained by selecting its protonated molecule (*m/z* 311) shows that the initial loss of HF occurs to a very small extent, producing ions at *m/z* 291 whose relative abundance is about 1%. For both compounds **3** and **4**, the most intense product ions are $[(M+H)-46]^+$ and, similarly to **1**, they are attributed to consecutive losses of H_2O and CO. Hydration of fragment ions is quite scarce for **4** and it occurs only for those at *m/z* 223, produced by a $C_2H_2N_2$ loss from $[(\mathbf{4}+H)-H_2O-CO]^+$ (*m/z* 265). Addition of one water molecule to the former ions produces the species at *m/z* 241.

When low-energy collision-induced dissociations occur in a triple quadrupole, different reaction pathways are activated in comparison with those detected in the ion trap: hydration reactions, which have great importance inside the ion trap, are undetectable in the QqQ regime. Furthermore, the possibility offered by the triple quadrupole of scanning the low *m/z* region allows one to detect product ions with low *m/z* values. Finally, MS^2 spectra obtained in the triple quadrupole generally

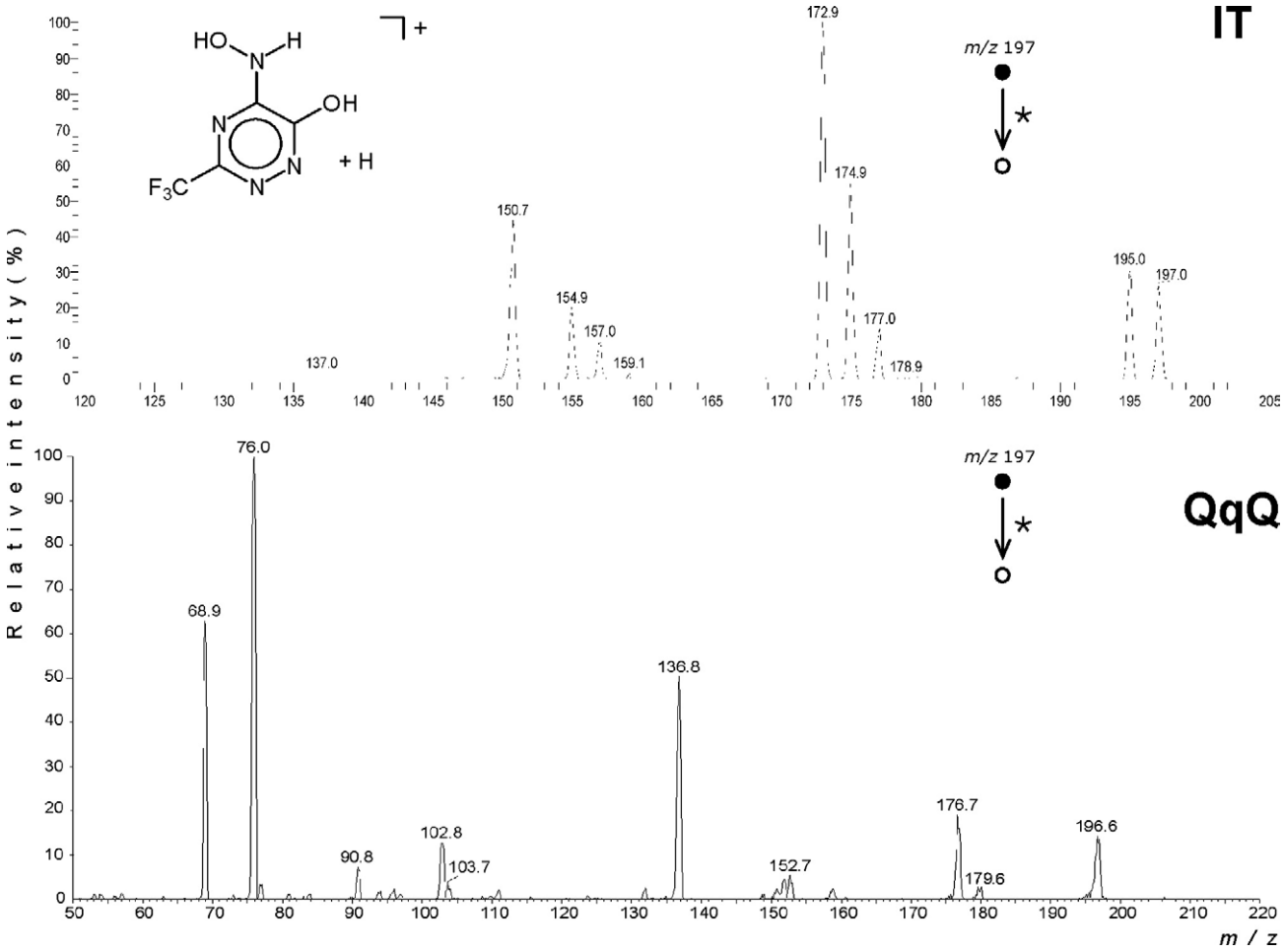

Figure 2. Comparison between ESI MS^2 product ion spectra of $[M+H]^+$ produced by **1** as a result of low-energy collision-induced dissociations occurring in a quadrupole ion trap (top) and in a triple quadrupole (bottom).

show a greater abundance of product ions than those produced in the ion trap.

The QqQ-MS^2 spectrum of $[\mathbf{1}+H]^+$ is reported in Figure 2 (bottom). The two most intense product ions are at *m/z* 69 and 76 that can be attributed to $C_2HN_2O^+/CF_3^+$ and F_2C^+—C≡N, respectively. The product ions at *m/z* 137, also detected in the ion trap but with a very low abundance (Figure 2, top), constitute abundant CID product ions formed in the QqQ instrument. Accurate mass measurements have shown that they are attributed to elimination of three molecule of hydrofluoric acid from the protonated molecule. Although elimination of the first molecule of HF produces intense ions at *m/z* 177, the successive loss of HF is undetectable, suggesting that the species $[(\mathbf{1}+H)-2HF]^+$ eliminates a further HF molecule with a very fast kinetics. In addition, the elimination of three HF molecules requires rearrangement of at least two hydrogen atoms.

The QqQ-MS^2 spectrum of **1** also shows the presence of the species at *m/z* 180, with a relative abundance of about 3%, which is much lower when low-energy collisions occur in the ion trap (Figure 2). These ions are due to loss of 17 u from $[M+H]^+$ and are formed by compounds **1**, **3**, and **4**, all of them bearing an oxygen atom at position 6 of the triazine ring. Accurate mass measurements have established that they are due to elimination of ·OH from the protonated molecules. It means that radical cation species, i.e., $[(M+H)-OH]^{+\bullet}$, rarely observed under electrospray conditions [16], are produced as a result of low-energy CID.

The QqQ-MS^2 spectra of $[\mathbf{2}+H]^+$ and $[\mathbf{3}+H]^+$ are compared in Figure 3. Regarding compound **2**, product ions common to those produced inside the ion trap are at *m/z* 239 ($[(M+H)-H_2O]^+$), 219 ($[(M+H-H_2O)-HF]^+$), 191 (219−N_2), and 144 ($[(M+H-H_2O)-CF_3CN]^+$), whose elemental compositions have been confirmed by accurate mass measurements.

The ions at *m/z* 144 have a high intensity in the QqQ-MS^2 spectrum, with a relative intensity of about 93%, whereas it is 30% in the IT-MS^2 spectrum. These are yielded by elimination of CF_3CN from the species $[M+H-H_2O]^+$. This decomposition pathway is specific for **2** and it is not observed for all the other compounds. Low *m/z* ions are undetectable in the ion trap, whereas they are very abundant in the QqQ-MS^2 spectrum of **2**,

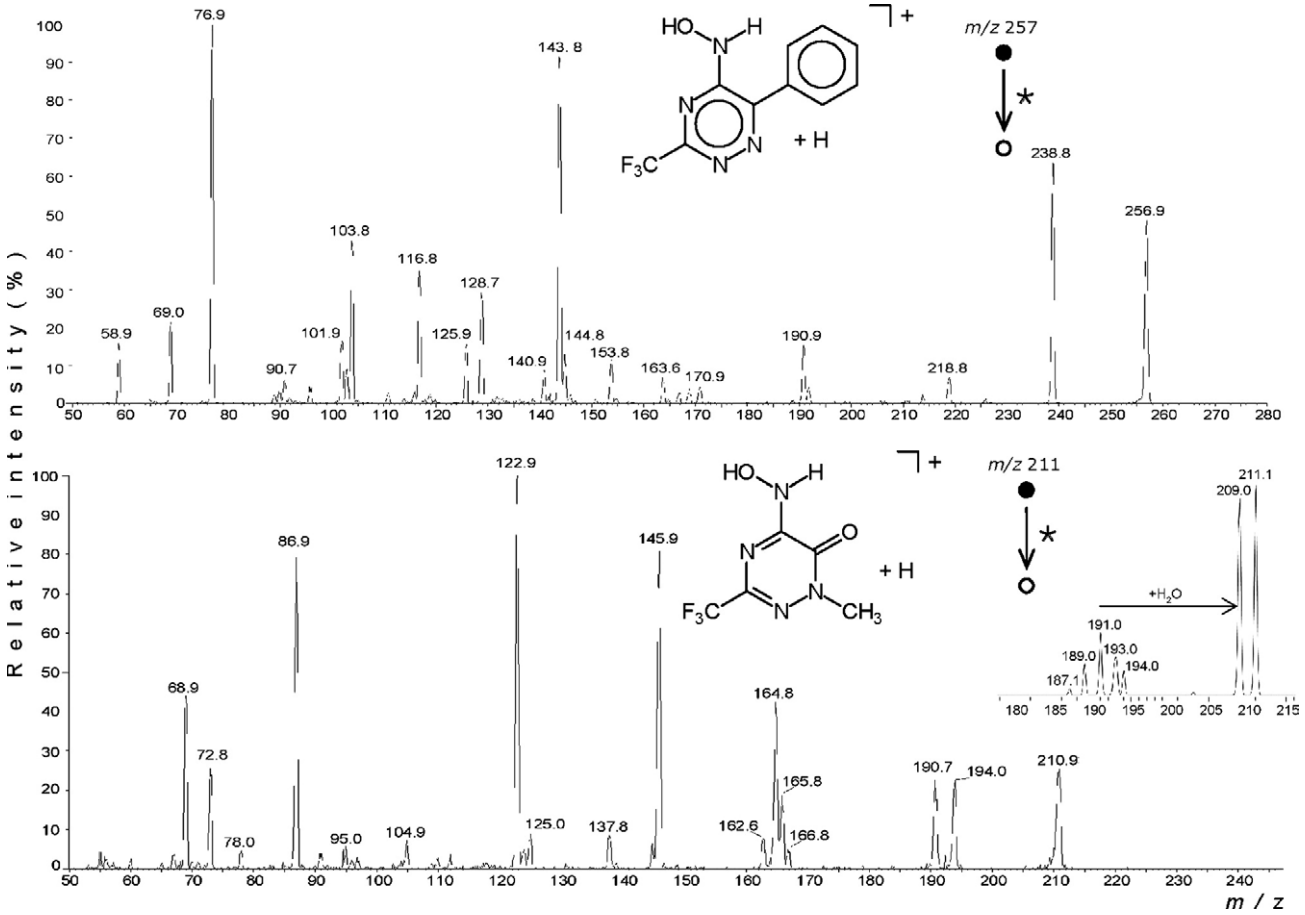

Figure 3. ESI QqQ-MS^2 product ion spectra obtained as a result of low-energy collision-induced dissociations for protonated **2** (top) and **3** (bottom). A portion of the IT-MS^2 mass spectrum of protonated **3** is reported in the inset.

whose base peak is at *m/z* 77 (Figure 3, top). Because analogous ions are not formed by the other compounds, those at *m/z* 77 can be attributed to the phenyl cation. Other product ions present both in the IT-MS^2 and QqQ-MS^2 spectra are at *m/z* 104, 117, and 129. They have been attributed to $[C_7H_6N]^+$, $[C_7H_5N_2]^+$, and $[C_8H_5N_2]^+$, respectively.

However, differently by its IT-MS^2 spectrum—which shows a very scarce fragmentation—the QqQ-MS^2 spectrum of protonated **3** shows a wide variety of ions (Figure 3, bottom). Those at *m/z* 123 (100%), 87 (80%), and 146 (83%) are the most abundant ones. Their origin and composition have been determined by MS^n measurements in the ion trap and by accurate mass measurements. $[\mathbf{3}+H]^+$ can eliminate HF or, alternatively, water and CO, yielding the species at *m/z* 191 and 165, respectively. This latter can follow two distinctive decomposition pathways: one consists of the elimination of CH_2N_2, thus forming ions at *m/z* 123, as shown by IT-MS^3 measurements. Alternatively, through consecutive eliminations of N_2 and CF_2, ions at *m/z* 165 can yield the cations at *m/z* 87. As already observed for **1**, **3** and **4** also show a prominent loss of a hydroxyl radical that in all cases is much more abundant when CIDs occur in the triple quadrupole than in the ion trap. The species $[(\mathbf{3}+H)-OH]^{+\bullet}$ have an *m/z* value equal to 194. In the IT-MS^2 and QqQ-MS^2 product ion spectra their relative intensities are about 5 and 20%, respectively (Figure 3, bottom and inset).

As a result of CID occurring in the triple quadrupole, $[\mathbf{4}+H]^+$ decomposes through the elimination of a hydroxyl radical, whereas other first-generation product ions are not observed. The resulting ions $[(\mathbf{4}+H)-OH]^{+\bullet}$ have a relative intensity of about 18%. These odd-electron cations may follow two decomposition routes, both involving elimination of radicals: in fact, the $\cdot CF_3$ and $HCO^{\bullet}$ species can be lost, yielding even-electron cations at *m/z* 225 and 265, respectively. These latter can lose a CH_2N_2 molecule producing the species at *m/z* 223 that constitute the most intense peak in the QqQ-MS^2 spectrum of $[\mathbf{4}+H]^+$. Fragmentation pathways of $[\mathbf{4}+H]^+$ occurring both in the ion trap and in the QqQ mass spectrometer are reported in Scheme **2**.

*Gas-Phase Behavior of Anions Produced by ESI of Compounds **1–4***

Deprotonated molecules $[M-H]^-$ of compounds **1–4** have been produced by electrospray ionization and

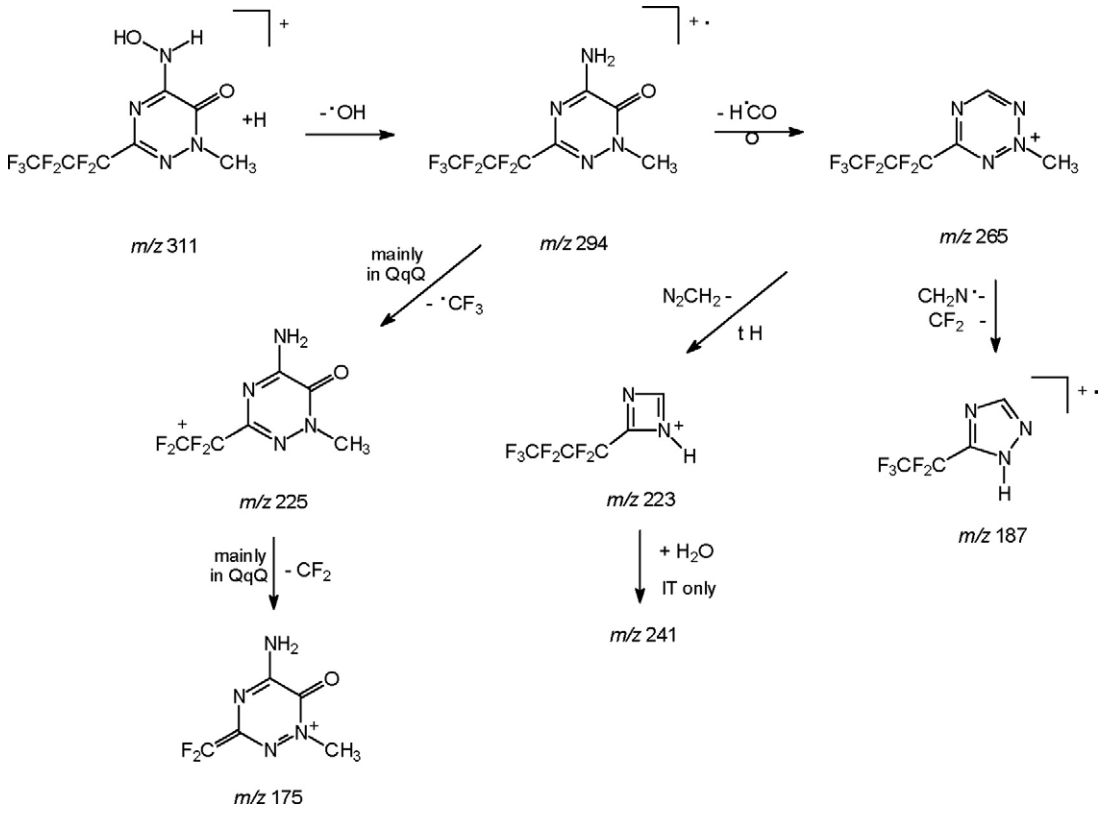

Scheme 2.

studied both in an ion trap and in a triple quadrupole instrument. In comparison with protonated molecules, two main differences can be highlighted in their gas-phase behavior: (1) hydration reactions, observed for cations in IT-MS^2 experiments, do not occur for anions; and (2) successive eliminations of HF, which are important gas-phase decompositions of cations, are not observed for anions.

Decomposition reactions of deprotonated molecules of compounds **1–4** are initiated by loss of a hydroxyl radical and proceed through eliminations of neutral species (Figure 4). It follows that most product ions formed as a result of MS^n experiments are radical anions. Some examples of radical anions produced by ESI have been described for glycosides [17, 18], nitro compounds [19, 20], diuretics [21], and others.

The IT-MS^2 spectrum of $[\mathbf{1}-H]^-$ (*m/z* 195) shows a prominent loss of 17 u yielding the most abundant ions at *m/z* 178. Accurate mass measurements have confirmed that they are due to the loss of a $^{\bullet}OH$ radical. Theoretical calculations, carried out on **1** deprotonated at different atoms, have shown that proton abstraction is more favored from the hydroxyl group in position 6 of the triazine ring, followed by the nitrogen and the oxygen of the hydroxylamino moiety (Figure 1, bottom row and Table 1). By considering the large energy difference, deprotonation at the hydroxylamino oxygen atom is highly unfavored.

When radical anions $[(\mathbf{1}-H)-OH]^{-\bullet}$ are selected as precursors for MS^3 measurements in the ion trap, two product ions are detected: one at *m/z* 150 (100%) and another at *m/z* 151 (18%). The use of the Orbitrap allowed us to determine that they are produced by losses of CO and HCN, respectively. Elimination of N_2 occurs only from the ions at *m/z* 150, as shown by MS^4 measurements.

Similarly, the QqQ-MS^2 spectrum of $[\mathbf{1}-H]^-$ shows a prominent loss of 17 u, but the most abundant ions are at *m/z* 150, already described for the ion trap. All the QqQ-MS^2 spectra produced by the species $[M-H]^-$ of compounds **1–4** show abundant ions at *m/z* 66 that are undetectable in MS^2 spectra obtained by the ion trap. When these latter ions are produced in the ESI source by CID in source fragmentation and detected by the Orbitrap, the most probable elemental composition was C_2N_3. By considering the molecular structure of compounds **1–4**, the formation of this species should require important rearrangement reactions in their skeleton.

The IT-MS^2 spectrum of $[\mathbf{2}-H]^-$ (*m/z* 255) shows the most intense ions at *m/z* 237 (Figure 4, top). An accurate examination of the spectrum reveals that it has a shoulder on the right side. Indeed, high-resolution, accurate mass measurements show two peaks at *m/z* 238.0470 and 237.0392, with 28:100 intensity ratio, due to losses of $^{\bullet}OH$ and water, respectively. Thus, for the deprotonated molecule $[\mathbf{2}-H]^-$, the elimination of wa-

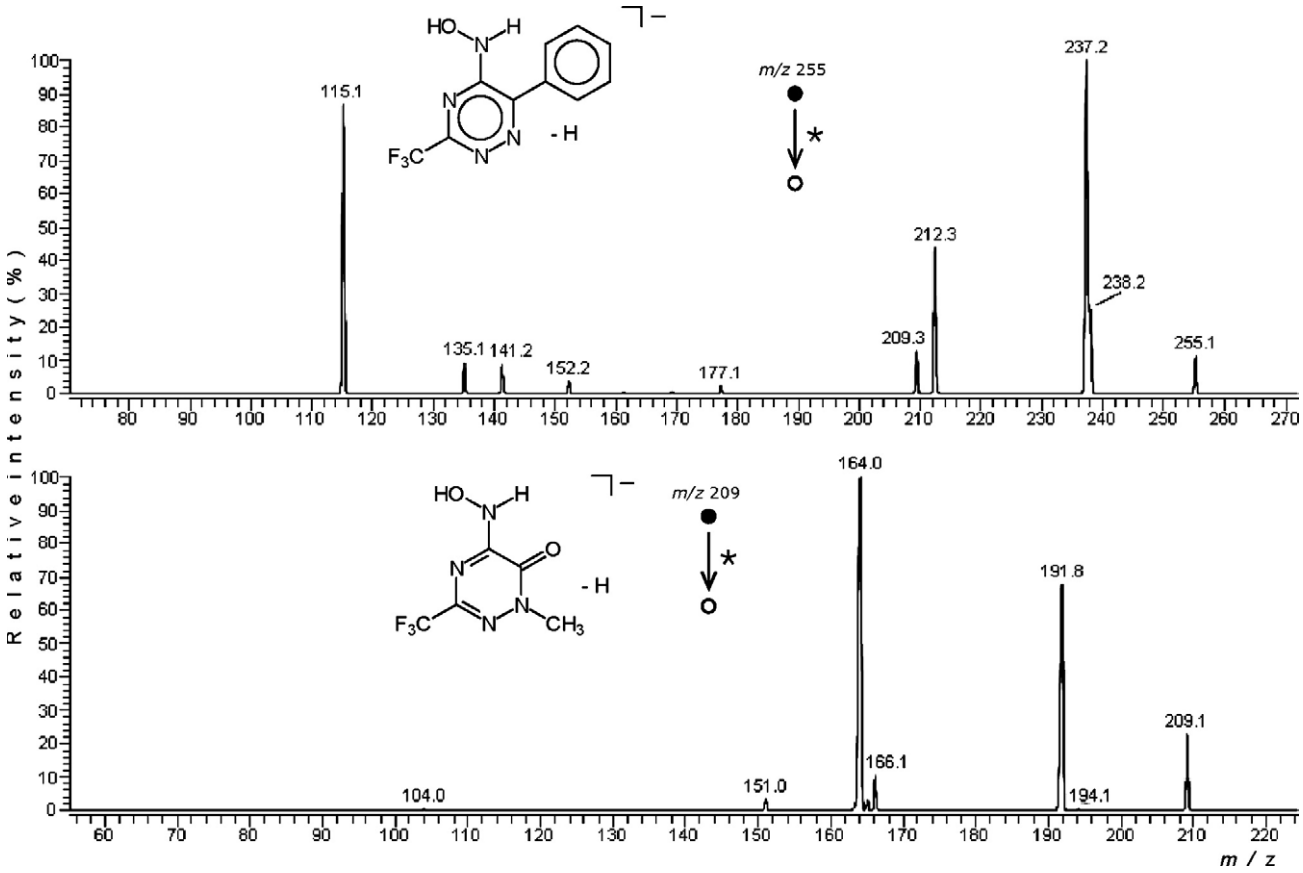

Figure 4. ESI IT-MS^2 product ion spectra obtained for deprotonated **2** (top) and **3** (bottom).

ter is much higher than that of $^{\bullet}$OH. Similarly to positive ions, the proximity effect of the pendant phenyl to the hydroxylamino group is the driving force for the elimination of water with the formation of a tricyclic system, thus suggesting that deprotonation does not involve the exocyclic OH group. In turn, ions $[(\mathbf{2}-H)-H_2O]^-$ can lose N_2, yielding the species at *m/z* 209. Distinctively from the other deprotonated compounds, $[\mathbf{2}-H]^-$ may fragment through elimination of isocyanic acid (HOCN) forming ions at *m/z* 212. The formation of both ions at *m/z* 212 and 209 occurs exclusively inside the ion trap. Other abundant ions present in the IT-MS^2 product ion spectrum of $[\mathbf{2}-H]^-$ are at *m/z* 115 (Figure 4, top), due to the radical anion $C_8H_5N^{-\bullet}$ (calcd 115.0427, measured 115.0426), reasonably containing the exocyclic nitrogen atom.

Similarly to that occurring in the ion trap, the QqQ-MS^2 product ion spectrum of $[\mathbf{2}-H]^-$ shows abundant ions at *m/z* 115 that in this case constitute the base peak. On the contrary, elimination of a hydroxyl group is unfavored in the triple quadrupole because it results from the relative abundance (8%) of ions at *m/z* 237, whereas the loss of water is undetectable.

Elimination of $^{\bullet}$OH is a major decomposition reaction also occurring in the ion trap for $[\mathbf{3}-H]^-$, yielding ions at *m/z* 192 (Figure 4, bottom). These latter further decompose by elimination of CO thus producing the species at *m/z* 164 that constitute the most intense peak in the MS^2 spectra obtained both by IT and QqQ mass spectrometers (Figure 4, bottom, and Scheme **3**). Because the ions at *m/z* 192 are undetectable when collision-induced dissociations occur in the triple quadrupole, it follows that they lose CO with a kinetics faster than the flight time of the ions in the QqQ system.

After elimination of OH$^{\bullet}$ and CO, the decomposition pathways involve the loss of 28 u, which accurate mass

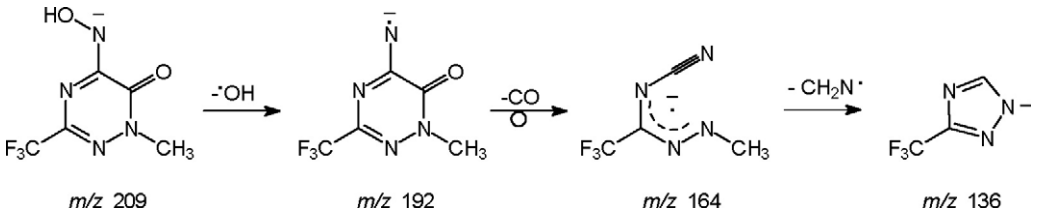

Scheme 3.

measurements showed to be attributable to CH_2N_2. The ions so formed (i.e., *m/z* 136) have high abundance (90%) in the QqQ-MS^2 spectrum, whereas in the ion trap they are detectable only as a result of MS^3 of the species at *m/z* 164 (Scheme **3**).

The gas-phase behavior of $[\mathbf{4}-H]^-$ strictly resembles that of $[\mathbf{3}-H]^-$, with analogous ions but shifted by 100 u. The only significant difference between them is the abundance of the $[(M-H)-OH]^{-\bullet}$ ions in their corresponding IT-MS^2 spectra: it is 70% for $[\mathbf{3}-H]^-$ (Figure 4, bottom) and only 1% for $[\mathbf{4}-H]^-$. Also their QqQ-MS^2 spectra are similar, but the abundance of the ions $[(M-H)-OH-CO-CH_2N]^{-\bullet}$ is much higher for **3** (*m/z* 136, 95%) than for **4** (*m/z* 236, 20%).

Conclusion

This study has allowed us to investigate the gas-phase ion chemistry of a new series of fluorinated 1,2,4-triazines. The decomposition pathways of protonated and deprotonated molecules, occurring as a result of low-energy collision-induced dissociations in an ion trap and in a QqQ mass spectrometer, have shown interesting features depending on the nature and structure of precursor ions. The use of high-resolution, accurate mass measurements, MS^n experiments, and theoretical calculations allowed us to define both the nature and the composition of product ions formed in their decomposition pathways. The occurrence of elimination/hydration reactions followed by positive ions in the ion trap is noteworthy. These reactions, which consist of elimination of HF molecules and addition of water, cause the formation of puzzling ions, differing 2 u from each other, in the IT-MS^n spectra. Loss of a hydroxyl radical from species $[M+H]^+$ also occurs; it is more abundant in the QqQ-MS^2 spectra than in the IT-MS^2 spectra.

Low-energy collision-induced dissociations of deprotonated molecules are dominated by odd-electron anions whose formation is initiated by loss of a hydroxyl radical from $[M-H]^-$.

This study has shown that the combination of different experimental and theoretical approaches is a useful tool for investigating gas-phase ion chemistry of heterocyclic compounds such as fluorinated triazines.

Acknowledgments

The authors gratefully acknowledge financial support through the Italian MIUR within the National Research Project "Dalle singole molecole a complessi e nanostrutture: struttura, chiralità, reattività e teoria" (PRIN 2006) and the Universities of Siena and Palermo.

References

1. Ronchi, S.; Prosperi, D.; Compostella, F.; Panza, L. Synthesis of Novel Carborane-Hybrids Based on a Triazine Scaffold for Boron Neutron Capture Therapy. *Synlett* **2004,** 1007–1010.
2. Oliva, J. M.; Azenha, E. M. D. G.; Burrows, H. D.; Coimbra, R.; de Melo, J. S. S.; Canle, M. L.; Fernandez, M. I.; Santaballa, J. A.; Serrano-Andres, L. On the Low-lying Excited States of Sym-Triazine-based Herbicides. *Chem Phys Chem*. **2005,** *6,* 306–314.
3. Filler, R.; Kobayashi, Y.; Yagupolskii, L. M. *Organofluorine Compounds in Medicinal Chemistry and Biomedical Applications*. Amsterdam: Elsevier, 1993.
4. (a) Chambers, R. D.; Sargent, C. R. Polyfluoroheteroaromatic Compounds. *Adv. Heterocycl. Chem*. **1981,** *28*, 1–71; (b) Differding, E.; Frick, W.; Lang, R. W.; Martin, P.; Schmit, C.; Veenstra, S.; Greuter, H. Fluorinated Heterocycles: Targets in the Search for Bioactive Compounds and Tools for Their Preparation. *Bull. Soc. Chim. Belg*. **1990,** *99*, 647–671; (c) Silvester, M. J. Recent Advances in Fluoroheterocyclic Chemistry. *Adv. Heterocycl. Chem*. **1994,** *59*, 1–38; (d) Burger, K.; Wucherpfennig, U.; Brunner, E. Fluoro Heterocycles with Five-membered Rings. *Adv. Heterocycl. Chem*. **1994,** *60*, 1–64; (e) Furin, G. G. Syntheses of Heterocyclic Compounds with Perfluoroalkyl Groups Based on Internal Perfluoroolefins. In: *Targets in Heterocyclic Systems*, Attanasi, O. A.; Spinelli, D., Eds.; Società Chimica Italiana: Rome, Italy, 1998; Vol. 2, pp 355–441; (f) Zhu, S. Z.; Wang, Y. L.; Peng, W. M.; Song, L. P.; Jin, G. F. Synthesis of Fluoroalkyl Substituted Heterocycles Using Fluorine-containing Building Blocks. *Curr. Org. Chem*. **2002,** *6*, 1057–1096.
5. Hu, X. P.; Chen, H. L.; Zheng, Z. Ferrocene-based Chiral Phosphine-Triazines: A New Family of Highly Efficient P,N Ligands for Asymmetric Catalysis. *Adv. Synth. Catal*. **2005,** *347,* 541–548.
6. Gamez, P.; Reedijk, J. 1,3,5-Triazine-based Synthons in Supramolecular Chemistry. *Eur. J. Inorg. Chem*. **2006,** *2006*(1), 29–42.
7. Giacomelli, G.; Porcheddu, A.; de Luca, L. [1,3,5]-Triazine: A Versatile Heterocycle in Current Applications of Organic Chemistry. *Curr. Org. Chem*. **2004,** *8,* 1497–1519.
8. Buscemi, S.; Pace, A.; Palumbo Piccionello, A.; Pibiri, I.; Vivona, N.; Giorgi, G.; Mazzanti, A.; Spinelli, D. Five-to-Six Membered Ring-Rearrangements in the Reaction of 5-Perfluoroalkyl-1,2,4-oxadiazoles with Hydrazine and Methylhydrazine. *J. Org. Chem*. **2006,** *71,* 8106–8113.
9. (a) Giorgi, G.; Salvini, L.; Ponticelli, F. Gas Phase Ion Chemistry of the Heterocyclic Isomers 3-Methyl-1,2-Benzisoxazole and 2-Methyl-1,3-Benzoxazole. *J. Am. Soc. Mass Spectrom*. **2004,** *15,* 1005–1013; (b) Giorgi, G.; Ponticelli, F. Structural Characterization and Regiochemical Differentiation of α-Cyanoethylindole Isomers in the Gas Phase. *J. Am. Soc. Mass Spectrom*. **2005,** *16,* 397–405.
10. Buscemi, S.; Pace, A.; Palumbo Piccionello, A.; Macaluso, G.; Vivona, N.; Spinelli, D.; Giorgi, G. Fluorinated Heterocyclic Compounds. An Effective Strategy for the Synthesis of Fluorinated *Z*-Oximes of 3-Perfluoroalkyl-6-phenyl-2*H*-1,2,4-triazin-5-ones *via* a Ring Enlargement Reaction of 3-Benzoyl-5-perfluoroalkyl-1,2,4-oxadiazoles and Hydrazine. *J. Org. Chem*. **2005,** *70,* 3288–3291.
11. Frisch, M. J.; Trucks, G. W.; Schlegel, H. B.; Scuseria, G. E.; Robb, M. A.; Cheeseman, J. R.; Montgomery, J. A., Jr.; Vreven, T.; Kudin, K. N.; Burant, J. C.; Millam, J. M.; Iyengar, S. S.; Tomasi, J.; Barone, V.; Mennucci, B.; Cossi, M.; Scalmani, G.; Rega, N.; Petersson, G. A.; Nakatsuji, H.; Hada, M.; Ehara, M.; Toyota, K.; Fukuda, R.; Hasegawa, J.; Ishida, M.; Nakajima, T.; Honda, Y.; Kitao, O.; Nakai, H.; Klene, M.; Li, X.; Knox, J. E.; Hratchian, H. P.; Cross, J. B.; Bakken, V.; Adamo, C.; Jaramillo, J.; Gomperts, R.; Stratmann, R. E.; Yazyev, O.; Austin, A. J.; Cammi, R.; Pomelli, C.; Ochterski, J. W.; Ayala, P. Y.; Morokuma, K.; Voth, G. A.; Salvador, P.; Dannenberg, J. J.; Zakrzewski, V. G.; Dapprich, S.; Daniels, A. D.; Strain, M. C.; Farkas, O.; Malick, D. K.; Rabuck, A. D.; Raghavachari, K.; Foresman, J. B.; Ortiz, J. V.; Cui, Q.; Baboul, A. G.; Clifford, S.; Cioslowski, J.; Stefanov, B. B.; Liu, G.; Liashenko, A.; Piskorz, P.; Komaromi, I.; Martin, R. L.; Fox, D. J.; Keith, T.; Al-Laham, M. A.; Peng, C. Y.; Nanayakkara, A.; Challacombe, M.; Gill, P. M. W.; Johnson, B.; Chen, W.; Wong, M. W.; Gonzalez, C.; Pople, J. A. Gaussian 03, Revision D.02, Gaussian, Inc.: Wallingford, CT, 2004.
12. Becke, A. D. Density-functional Thermochemistry. III. The Role of Exact Exchange. *J. Chem. Phys.* **1993,** *98,* 5648–5652.
13. Callahan, M. P.; Crews, B.; Abo-Riziq, A.; Grace, L.; de Vries, M. S.; Gengeliczki, Z.; Holmes, T. M.; Hill, G. A. IR-UV Double Resonance Spectroscopy of Xanthine. *Phys. Chem. Chem. Phys*. **2007,** *9,* 4587–4591.
14. Giorgi, G.; Palumbo Piccionello, A.; Pace, A.; Buscemi, S. Hydration/Elimination Reactions of Trapped Protonated Fluoroalkyl Triazines. *J. Mass Spectrom*. **2008,** *43,* 265–268.
15. Thevis, M.; Kohler, M.; Schlörer, N.; Schänzera, W. Gas Phase Reaction of Substituted Isoquinolines to Carboxylic Acids in Ion Trap and Triple Quadrupole Mass Spectrometers after Electrospray Ionization and Collision-induced Dissociation. *J. Am. Soc. Mass Spectrom*. **2008,** *19,* 151–158.
16. Vessecchi, R.; Crotti, A. E. M.; Guaratini, T.; Colepicolo, P.; Galembeck, S. E.; Lopes, N. P. Radical Ion Generation Processes of Organic Compounds in Electrospray Ionization Mass Spectrometry. *Mini-Rev. Org. Chem*. **2007,** *4,* 75–87.
17. Cuyckens, F.; Claeys, M. Determination of the Glycosylation Site in Flavonoid Mono-O-Glycosides by Collision-induced Dissociation of Electrospray-Generated Deprotonated and Sodiated Molecules. *J. Mass Spectrom*. **2005,** *40,* 364–372.
18. Es-Safi, N.-E.; Kerhoas, L.; Ducrot, P.-H. Application of Positive and Negative Electrospray Ionization, Collision-induced Dissociation and Tandem Mass Spectrometry to a Study of the Fragmentation of 6-Hydroxyluteolin 7-*O*-glucoside and 7-*O*-glucosyl-(1→3)-glucoside. *Rapid Commun. Mass Spectrom.* **2005,** *19*, 2734–2742.
19. Justes, D. R.; Talaty, N.; Cotte-Rodriguez, I.; Cooks, R. G. Detection of Explosives on Skin Using Ambient Ionization Mass Spectrometry. *Chem. Commun*. **2007,** *33*, 2142–2144.

20. Danikiewicz, W.; Bienkowski, T.; Wojciechowski, K. Application of Electrospray Ionization Mass Spectrometry for Studies of Anionic *o*-Adducts of Aromatic Nitrocompounds. *Tetrahedron Lett*. **2004,** *45*, 931–934.

21. Thevis, M.; Schänzer, W.; Schmickler, H. Effect of the Location of Hydrogen Abstraction on the Fragmentation of Diuretics in Negative Electrospray Ionization Mass Spectrometry. *J. Am. Soc. Mass Spectrom*. **2003,** *14,* 658–670.